View metadata, citation and similar papers at core.ac.uk

brought to you by CORE

provided by Hydraulic Engineering Repository

HENRY

Hydraulic Engineering Repository

Ein Service der Bundesanstalt für Wasserbau

Conference Paper, Published Version

Faruque, M. A. A.; Sarthi, Partha; Balachandar, Ram

Scour by submerged three-dimensional wall jets

Verfügbar unter/Available at: https://hdl.handle.net/20.500.11970/100016

Vorgeschlagene Zitierweise/Suggested citation:
Faruque, M. A. A.; Sarthi, Partha; Balachandar, Ram (2006): Scour by submerged three-dimensional wall jets. In: Verheij, H.J.; Hoffmans, Gijs J. (Hg.): Proceedings 3rd International Conference on Scour and Erosion (ICSE-3). November 1-3, 2006, Amsterdam, The Netherlands. Gouda (NL): CURNET. S. 204-213.

Standardnutzungsbedingungen/Terms of Use:

Die Dokumente in HENRY stehen unter der Creative Commons Lizenz CC BY 4.0, sofern keine abweichenden Nutzungsbedingungen getroffen wurden. Damit ist sowohl die kommerzielle Nutzung als auch das Teilen, die Weiterbearbeitung und Speicherung erlaubt. Das Verwenden und das Bearbeiten stehen unter der Bedingung der Namensnennung. Im Einzelfall kann eine restriktivere Lizenz gelten; dann gelten abweichend von den obigen Nutzungsbedingungen die in der dort genannten Lizenz gewährten Nutzungsrechte.

Documents in HENRY are made available under the Creative Commons License CC BY 4.0, if no other license is applicable. Under CC BY 4.0 commercial use and sharing, remixing, transforming, and building upon the material of the work is permitted. In some cases a different, more restrictive license may apply; if applicable the terms of the restrictive license will be binding.

Scour by submerged three-dimensional wall jets

M.A.A. Faruque[1], Partha Sarathi[2] and Ram Balachandar[3]

[1]Research Associate, Department of Civil & Environmental Engineering, University of Windsor, Windsor, Ontario, Canada.

[2]Graduate Student, Department of Civil Engineering, University of Western Ontario, London, Ontario, Canada.

[3]Professor, Department of Civil & Environmental Engineering, University of Windsor, Windsor, Ontario, Canada.

The characteristics of scour caused by submerged square jets were studied by varying the densimetric Froude number, sediment grain size and tailwater conditions. Velocity measurements were conducted using a laser Doppler anemometer. Progressing from the start of the test towards asymptotic conditions, the geometric parameters used to describe scour are found to be sensitive to tailwater conditions and the ratio of the nozzle size-to-grain size. The present results indicate that the effect of nozzle size-to-grain size ratio can be important and needs to be incorporated in the interpretation of scour. This effect is reduced as asymptotic conditions are reached. Turbulent bursts were noted to have an important role in the scour process, and are more distinguishable with the finer bed material. At low values of the relative tailwater depth, the flow and the corresponding scour pattern tends to be non-symmetrical. Moreover, at low values of tailwater depth and higher densimetric Froude number, the scour pattern is quite different from the other test conditions.

I. INTRODUCTION

The prediction and control of scour is considered to be very important in hydraulic engineering practice. Flow through a hydraulic structure often issues in the form of a jet. To better understand the scouring process, jets interacting with sand beds have been studied by previous researchers and empirical relations have been proposed to predict scour. The jet configurations have varied from two-dimensional plane conditions to more complex geometry. Scour by three-dimensional (3-D) wall jets has not been studied as extensively as that caused by plane wall jets. Ref. [8] studied the scour produced by circular wall jets interacting with erodible sand and polystyrene beds. Using both air and water jets, they concluded that the main geometric characteristics of the scour hole are function of the densimetric Froude number ($F_o = U_o \Big/ \sqrt{g(\Delta\rho/\rho)d_{50}}$). Here, g is the acceleration due to gravity, ρ is the mass density of water, $\Delta\rho$ is mass density difference between the bed particle and fluid, and d_{50} is the median bed particle grain size. Using circular jets, Ref. [9] performed experiments with low tailwater depths. Noting the ridge to be flat at low tailwater depths, they concluded that the relative tailwater depth and width of the downstream channel do not affect the maximum depth of scour, whereas the location of the maximum scour was affected. The effect of tailwater depth has also been studied by Ref. [2]. They noted that tailwater has an influence on the maximum depth of scour at asymptotic conditions in the range $2.9 < F_o < 12$. They recognized a critical tailwater condition beyond which a decrease or increase in tailwater causes an increase in the maximum depth of scour. In addition, their data indicates that this critical value increases with increasing F_o and the effect of tailwater becomes insignificant when H/b_o is beyond 16. Sediment non-uniformity also has an effect on scour development by 3-D jets. In studying scour of the non-uniform sand beds, Ref. [7] noted that during early stages of the scouring process, the finer particles become suspended while the coarser particles move in sliding and saltation modes. These types of motions cause the formation of an armor surface that protects the bed as the scour hole develops.

Ref. [6] studied the effect of the channel width-to-nozzle width ratio (expansion ratio) on the scour development and observed that the scour depth was not affected when the expansion ratio is ten or greater. Ref. [4] studied local scour by deeply submerged circular jets of both air and water. They expected that the ratio of the size of the nozzle to the sand particle size should have an influence on the scour profiles, but did not elaborate further.

Ref. [1] compiled data from thirteen different sources including their own study and further highlighted F_o as a characteristic parameter to describe the scour profile. They noted that the tailwater depth had a pronounced effect on asymptotic scour depth for $F_o > 10$. The maximum depth of scour was larger at deeper submergences and higher values of F_o. It was also noted that to attain an asymptotic state at higher values of F_o, a longer time was required. Ref. [5] studied the effect of tailwater depth on local scour by wall jets using a 76 mm square nozzle. The tailwater depth varied from two to six times of nozzle opening and the nozzle expansion ratio was 14.5. In addition, a few exploratory tests were conducted at a nozzle expansion ratio of 41.3. Their data indicates that the maximum depth of scour tends to be larger at a lower submergence. At their lowest tailwater depth, they observed the formation of a secondary ridge that was attributed to secondary flow and proximity of the channel wall to the scour region. They suggested a series of scaling parameters consisting of nozzle size, sand grain size, and densimetric Froude number to describe the scour parameters. Finally, they concluded that the densimetric Froude number, tailwater depth and nozzle size-to-grain size ratio, all have an influence on the extent of scour caused by 3-D jets. They speculated about the dominance of each parameter at different flow conditions.

It is clear that the effects of tailwater depth, nozzle size, jet expansion ratio and grain size have to be clarified. Particularly the effect of nozzle size-to-grain size ratio has not been explicitly considered in previous analysis. In this paper, an effort is made to better understand the scouring process using the data from a

series of experiments with square wall jets. The variables of interest are the densimetric Froude number (F_o), tailwater depth (H) and sediment size (d_{50}). To this end, three different values of F_o (= 3.9, 6.6 and 10.0), a range of H/b_o ($1 \le H/b_o \le 18$) and two different values of b_o/d_{50} (= 10.8 and 37.5) were chosen.

II. Experimental Setup and Procedure

Experiments were carried out in a rectangular open channel flume at the University of Windsor. The nozzle was positioned near the upstream end of the flume. Flow straightners were used at the entrance to the nozzle to reduce the turbulence level and condition the flow. The square nozzle exit was 26.6 mm x 26.6 mm, which provides a nozzle area contraction of 131:1. The ratio of the channel width to the nozzle width was 41.3, which is well above the recommended value of ten to avoid side wall effects. Two types of sand were used in the experiments. The gradation measurements of the sands are tabulated in Table 1 and the bed material can be considered to be uniform.

TABLE 1: GRADATION MEASUREMENTS

Parameter	Sand 1	Sand 2
d_{50} (mm)	2.46	0.71
$\sigma_g = \sqrt{d_{84}/d_{16}}$	1.24	0.9

Table 2 provides the details of the experimental conditions. For measuring velocity, a single-component fiber-optic LDA was used. Due to the restrictions imposed by the geometry of the transmitting optics and the channel support structures, no measurements were possible at locations closer than a distance of one b_o (26.6 mm) downstream of the nozzle exit. Velocity measurements were conducted along the centerline of the nozzle at various stations ($1 \le x/b_o \le 25$). To measure the volume of the scour hole at asymptotic conditions, the procedure suggested by Ref. [2] was used. This involved neatly spreading out a thin sheet of plastic in the scour hole region and pouring known volumes of water until the water surface touched the tip of the point gauge, which was adjusted to the original sand bed level.

III. Results and Discussion

Visual observation:

Fig. 1 shows the schematic of the scour hole and ridge that is formed downstream of the nozzle. A general description of the scour process observed during the Test no. 318 (H/b_o = 18, d_{50} = 2.46 mm at F_o = 10) is first presented. Variations from this case at other flow conditions are described as the discussion progresses.

Once the pump was started, a vigorous scour action occurred close to the nozzle and formed a hole. At the early stages of the scouring process, the nearly elliptical scour hole grew longitudinally with a moving ridge formed downstream of the scour hole. The infant ridge moved forward with a rolling motion of sand particles and with time, the ridge became larger in size. The particles, which have already reached the crest of the ridge, slide down the downstream slope of the ridge. For the large tailwater, at no point, there was large scale suspension of sand particles into the flowing stream. Occasionally, particles could be seen to be thrown from the near bed region into the higher fluid velocity region away from the bed at the early stages of the experiment. In time, the scour hole and the ridge grew in size and the ridge was transported in the streamwise direction. For this grain size (d_{50} = 2.46 mm), after about 15 hours from the start of the test, the rate of change in the scour field was very much reduced and the geometry tended towards an asymptotic state.

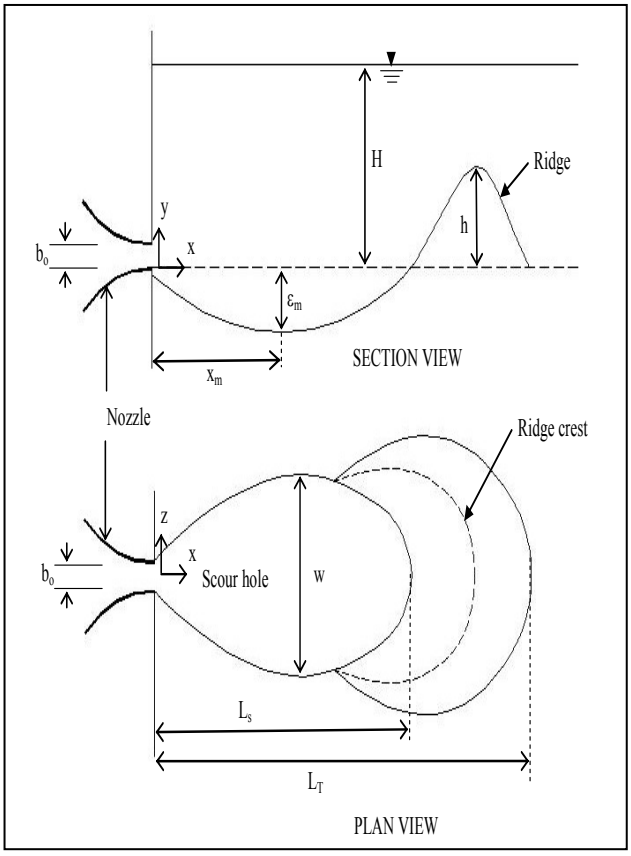

Fig. 1: Definition of scour parameters.

Fig. 2 provides a pictorial representation of the top view of the asymptotic scour hole and the ridge at different tailwater depths for F_o = 10. At the higher tailwater depths ($H/b_o \ge 4$), the scour hole and the ridge were almost symmetrical about the nozzle axis (Figs. 2a, 2b and 2c). With a decrease of tailwater depth ($H/b_o < 3$), the ridge crest disappeared and a plateau was formed on the ridge (Figs. 2e and 2f). At the lower values of H/b_o, confinement effects became important as the jet was constrained in the vertical motion. Due to this confinement, the jet expands more freely in the lateral direction, causing a larger sized hole in this direction and consequently, the ridge was also spread out more laterally. Dye visualization indicated higher velocity on the top portion of the ridge, compared to the other tailwater depths. As a result, the ridge tended to become flatter as the flow exerts sufficient shear stress to cause further movement of sand particles on the ridge. Moreover, at the lower tailwater depths, the scour hole and the ridge became non-symmetrical. This non-symmetrical nature was observed to be prevalent in the experiments with lower densimetric Froude numbers (F_o).

TABLE 2: DETAIL OF EXPERIMENTS

Test no.	U_o (m/s)	F_o	d_{50} (mm)	b_o (mm)	H/b_o	Run time (h)	$\varepsilon_{m\alpha}$ (mm)	w_α (mm)	$L_{s\alpha}$ (mm)	V_s (x 10^3 mm^3)
101	0.78	3.9	2.46	26.6	1	24	45.5	194	385	980
102	0.78	3.9	2.46	26.6	2	24	29.7	135	288	340
103	0.78	3.9	2.46	26.6	3	24	27.8	140	330	400
104	0.78	3.9	2.46	26.6	4	24	31.3	154	355	490
106	0.78	3.9	2.46	26.6	6	24	30.1	145	370	490
112	0.78	3.9	2.46	26.6	12	24	29.3	132	370	560
115	0.78	3.9	2.46	26.6	15	24	28.4	127	376	390
118	0.78	3.9	2.46	26.6	18	24	27.5	128	371	325
201	1.31	6.6	2.46	26.6	1	24	75.4	340	600	3340
202	1.31	6.6	2.46	26.6	2	24	69.9	259	585	3010
203	1.31	6.6	2.46	26.6	3	24	61.5	246	563	2320
204	1.31	6.6	2.46	26.6	4	24	60.1	228	546	2440
206	1.31	6.6	2.46	26.6	6	24	57.2	255	525	2320
212	1.31	6.6	2.46	26.6	12	24	61.9	248	550	2720
215	1.31	6.6	2.46	26.6	15	24	61.7	240	550	2600
218	1.31	6.6	2.46	26.6	18	24	58.7	234	539	2285
301	2.0	10.0	2.46	26.6	1	24	106.4	534	840	13370
302	2.0	10.0	2.46	26.6	2	24	106.1	420	830	11135
303	2.0	10.0	2.46	26.6	3	24	103.6	400	820	10500
304	2.0	10.0	2.46	26.6	4	24	95.7	410	795	9090
306	2.0	10.0	2.46	26.6	6	24	91.0	390	783	8950
312	2.0	10.0	2.46	26.6	12	24	93.9	368	780	8850
315	2.0	10.0	2.46	26.6	15	24	90.2	355	780	7830
318	2.0	10.0	2.46	26.6	18	24	92.4	367	790	8740
402	1.08	10.0	0.71	26.6	2	96	94.9	445	850	10000
404	1.08	10.0	0.71	26.6	4	96	89.0	454	810	9920
406	1.08	10.0	0.71	26.6	6	96	92.0	403	795	9490
418	1.08	10.0	0.71	26.6	18	96	90.1	397	783	8520
506	0.71	6.6	0.71	26.6	6	96	57.8	246	545	2600
518	0.71	6.6	0.71	26.6	18	96	58.0	238	570	2610
606	0.42	3.9	0.71	26.6	6	96	29.1	124	355	495

Note: The last two digits in the Test no. represent the tailwater ratio (H/b_o).

For the lower tailwater depths, the jet initially tended to move laterally to one side. However, with time the flow tended to become symmetrical about the nozzle axis and the scour hole and the ridge changed in response to the jet movement. Fig. 3 shows the scour pattern at $F_o = 6.6$ and $H/b_o = 2$. For this flow, the jet initially moved to the right of the centerline and then moved slowly towards the nozzle axis. The corresponding scour pattern reflects this phenomenon where the ridge is clearly non-symmetrical. Ref. [5] reported the presence of two secondary ridges on both sides of the main ridge in the experiment with a larger size nozzle ($b_o = 76$ mm) at $H/b_o = 2$, which was noted to be an effect of the jet expansion ratio (B/b_o). However, in the present study no secondary ridge was observed on either side of the main ridge. In their study, the jet expansion ratio was 14.5, whereas, for the present study, it is 41.3.

Visual observations also indicate the presence of turbulent bursts, which occurred frequently in the region downstream of the maximum depth of the scour hole. The importance of these burst events in scour studies have been pointed out recently by Ref. [3]. Few scattered bursts were also observed in the region upstream of the maximum depth of the scour hole. For experiments with the coarser sand ($d_{50} = 2.46$ mm), the turbulent bursts did not play a considerable role in sediment transport. The bursts were not strong enough to transport the larger particles and only a sweeping motion of the finer particles occurred. However, for the experiments with the finer sand ($d_{50} = 0.71$ mm), the frequency of the turbulent bursts was higher and visually appeared to play a considerable role in sediment transport. With the finer sand bed, in addition to the longitudinal growth of the scour hole and formation of the ridge, some particles were also transported as suspended load and were deposited past the ridge at the beginning of the experiment, and formed a rippled bed past the ridge. However, with time the scour hole and the ridge covered the uneven bed. After the formation of the ridge, a small

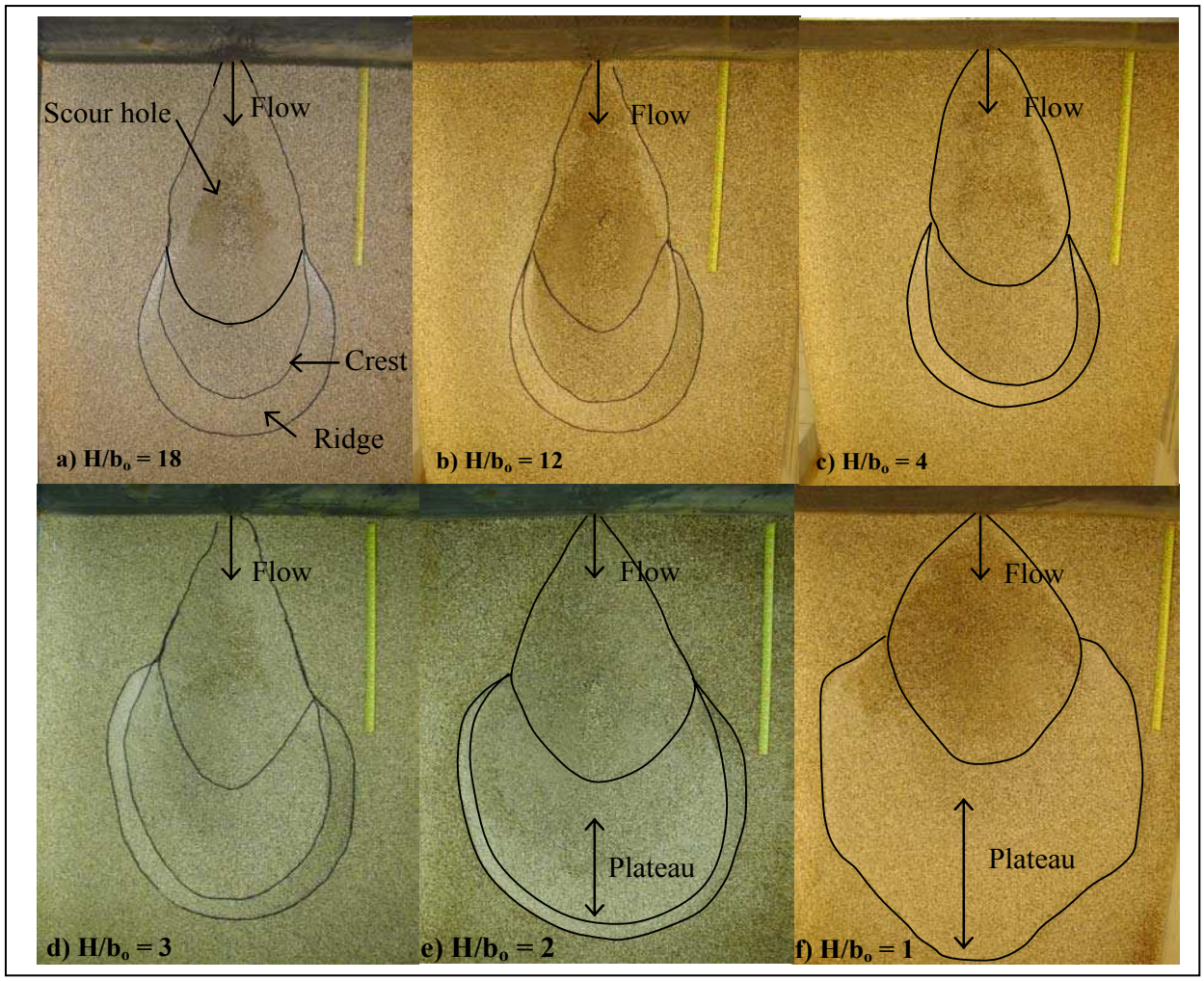

Fig.2: Top view of the scour hole and the ridge (F_o = 10).

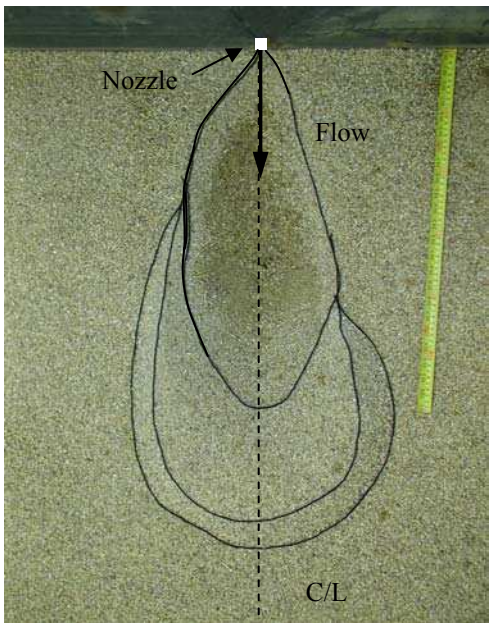

Fig. 3: Top view of the scour profile of Test no. 202 (F_o = 6.6, H/b_o = 2).

dune with a lateral curvature formed on the upstream slope of the ridge (see Fig. 4a). Over time, this dune migrates towards the crest (Figs. 4b, 4c) and falls off the crest. Soon, a second dune forms and begins to migrate up the ridge. Occasionally, due to the occurrence of turbulent bursts, the dune broke up (Fig. 4d) and rolled down to the ridge towards the scour hole. The bursts were strong enough to cause rolling motion of particles in all directions. Some of the particles were seen to roll down towards the scour hole, while others were thrown past the ridge crest. The migrating dunes were not observed in the experiments with the coarser sand.

Scour progress with time:

Figs. 5a - c show the variation of maximum depth of the scour hole with increasing time at various tailwater and F_o values. In these figures, the data of Ref. [5] and Ref. [2] have also been included to enable comparison. Ref. [2] conducted experiments with a 51 mm square nozzle (F_o = 4.4, H/b_o = 1.57, b_o/d_{50} = 62.5, and B/b_o = 12). It should be remarked that the value of b_o/d_{50} in the present study is 10.8 and 37.5 for the coarser and the finer sand, respectively. Considering the three sets of data, it should be noted that the overall range of b_o/d_{50} and H/b_o are quite large. Furthermore, the range of expansion ratio

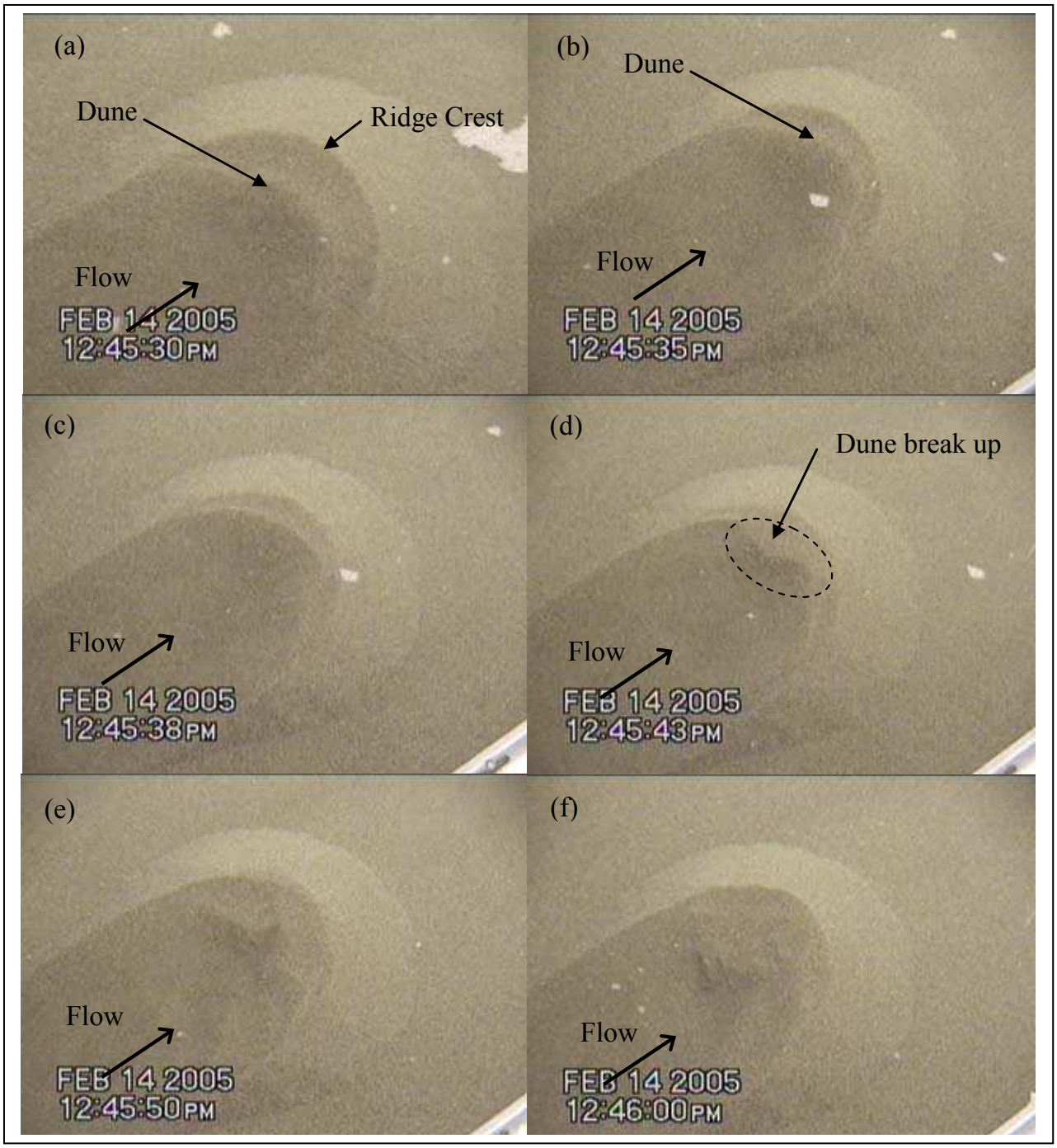

Fig. 4: Formation and rolling down of the small dune (Test no. 418).

is also quite varied ($12 \leq B/b_o \leq 41.3$). The present data at the lower value of F_o (= 3.9) is in agreement with that of Ref. [2] and Ref. [5], indicating that tailwater depth has no significant effect on the maximum depth of scour at low F_o, barring the data at the lowest tailwater condition ($H/b_o = 1$). For $H/b_o = 1$, it should be remarked that it was not visually possible to actually obtain the maximum depth of the scour during the progress of the test. Consequently, only the data at an asymptotic condition after the flow was stopped is shown in the figure. In fact, the present and previous data indicate that for $F_o < 5$, the influence of b_o/d_{50} is important during the early stages of scour and the maximum depth of the scour hole becomes almost independent of all other parameters at an asymptotic state (merging of curves A and B).

Fig. 5b shows the time variation of scour at $F_o = 6.6$. It can be seen from Fig. 5b that for $H/b_o \geq 3$, the data is more or less collapsed on to a single line (curve C). For $H/b_o \leq 2$, the maximum depth of scour is higher (curve D). This is principally due to the effect of tailwater as all other parameters are the same as in curve C and the value of B/b_o is very large in the present experiments. For $H/b_o \leq 2$, since the expansion of the jet and entrainment of ambient fluid is limited in the vertical direction towards the free surface, the jet diffusion is reduced and has more

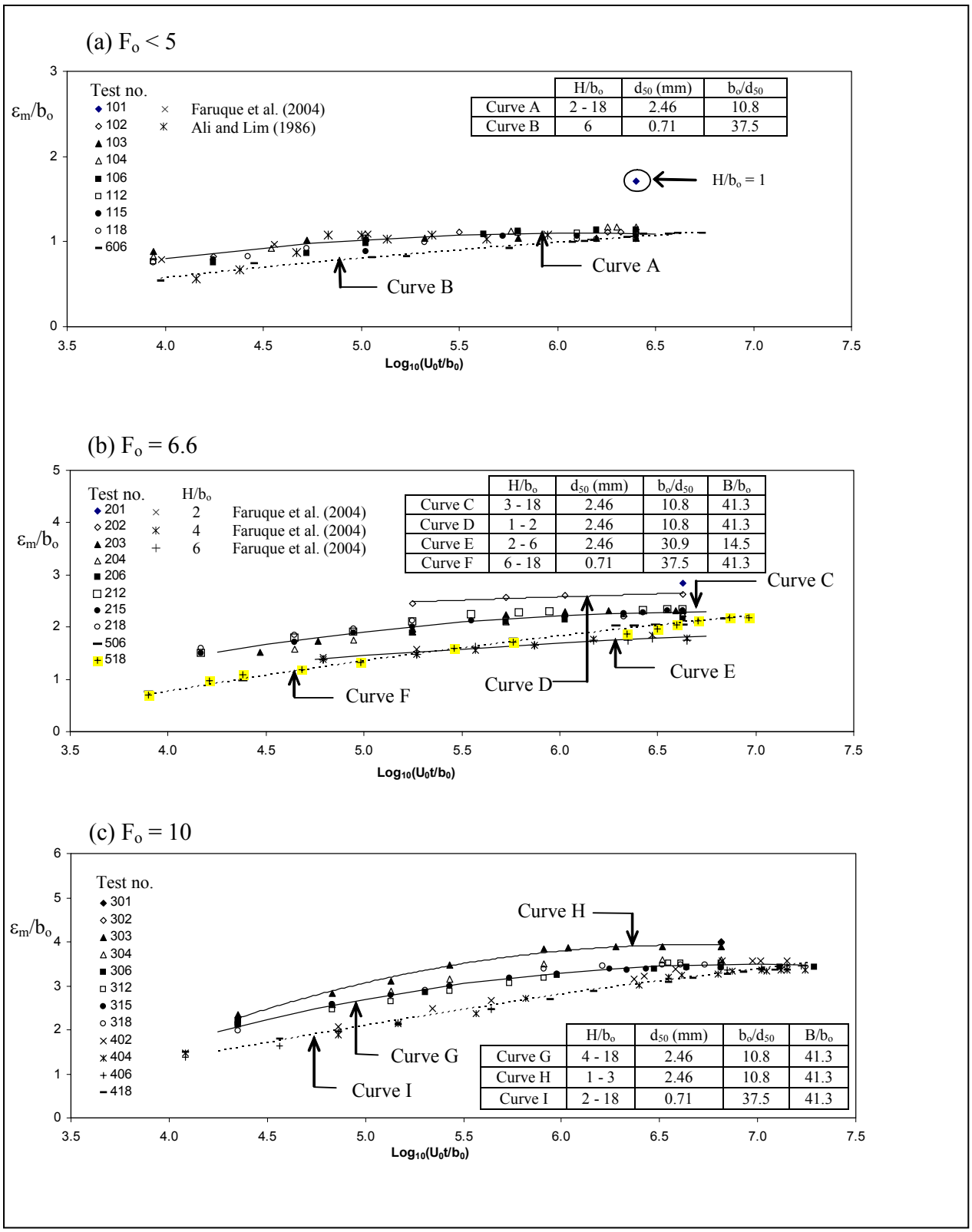

Fig. 5: Variation of maximum depth of the scour with time.

potential to cause scour. It is important to note that the data of Ref. [5] obtained with a 76 mm square nozzle and b_o/d_{50} = 30.9, though collapsed together (curve E), are different from the present set of data. This could be due to the change in b_o/d_{50} or due to the expansion ratio (B/b_o), as both values are different from the present data set. Also shown in Fig. 5b is the data of the tests conducted with the smaller sand (d_{50} = 0.71 mm) and the trend is indicated by curve F (H/b_o = 6 and 18). Clearly, the evolution of scour with the finer sand follows a

distinct trend different from the larger sand. However, at asymptotic conditions, the maximum depth of scour is quite similar for both grain sizes. Since the expansion ratio is held constant and the tailwater depths are large, and only the sand bed is changed, one can conclude that the difference noted between curves C and F is principally due to b_o/d_{50}. Comparing curves E and F, one can note that there is 21% change in b_o/d_{50}, whereas there is a 185% change in B/b_o. The difference noted in the two curves is more likely due to the changes in b_o/d_{50} as the expansion ratio is greater than ten and should have a minimal effect (Ref. [6]). Given that all the data presented in Fig. 5b are from tests conducted at larger values of B/b_o, one is tempted to conclude that the effect of b_o/d_{50} can be quite important in the interpretation of the results. Previous studies have qualitatively speculated on the importance of b_o/d_{50} (Ref. [4]). This is perhaps, the first quantitative study to identify the role of b_o/d_{50}. With increasing b_o/d_{50}, one can note that the time to attain an asymptotic state is increased.

Fig. 5c shows the present data at $F_o = 10$ and illustrates that for the experiments with larger grain size and $H/b_o > 3$, the data are collapsed together on to a single line (curve G). The data of the experiments with smaller sand size are collapsed on to a different line (curve I). Since the value of F_o (= 10) is constant, the larger grain size tests were conducted at a higher velocity, which proportionally causes higher shear stresses near the bed and increases scour. It is important to recognize that as the expansion ratio is held constant in the tests denoted by curves G and I (but different b_o/d_{50}), the differences in the two curves can be attributed to the effect of nozzle size-to-grain size ratio.

Overall, one can note from Figs. 5a - c that there is a dependence of ε_m on tailwater depth, but it is limited to $H/b_o \leq 1$ for $F_o = 3.9$, $H/b_o \leq 2$ for $F_o = 6.6$, and at the highest value of F_o, the effect of tailwater is prominent for $H/b_o \leq 3$. Furthermore, Fig. 5 clearly shows that the effect of b_o/d_{50} can be important at all values of F_o.

The variation of the maximum width of the scour hole and the variation of the length of the scour hole with time for three values of F_o is available in Ref. [10] and details are avoided here for brevity.

Scour geometry at asymptotic conditions:

Fig. 6a shows the asymptotic scour profiles along the centerline of the nozzle for the experiments having different tailwater conditions at $F_o = 10$. In this figure, both the axes are normalized by the width of the nozzle (b_o). Only some of the profiles are shown to avoid cluttering. The profiles indicate that the location of maximum depth of the scour hole tends to be closer to the nozzle with decreasing tailwater depth. The height of the ridge was found to be larger with a sharp crest at the higher tailwater conditions ($H/b_o \geq 4$), while the ridge tends to flatten out with the decreasing tailwater depth. It is note worthy that at asymptotic conditions, the profiles for $H/b_o \geq 4$ are all collapsed together. Not only is the maximum depth of scour the same at the larger tailwater depths, but the entire scour profiles are similar.

The normalized asymptotic perimeter of the scour hole is shown in Fig. 6b. The location of maximum width of the scour hole tends to be closer to the nozzle and is wider at lower tailwater depths. The inability of the jet to expand in the vertical direction (towards the free surface) causes the jet to expand laterally. This results in the scour hole width being larger at $H/b_o = 1$ than at any other conditions. Fig. 6c shows the normalised asymptotic perimeter of the ridge for the experiments shown in the earlier figures. The ridge is wider at lower tailwater depths. Moreover, the shape of the ridge is different at $H/b_o = 1$. Initially, at the start of the test with low H/b_o, the shape of the ridge is very similar to that of the other tailwater depths. However, with increased lateral spreading of the jet, the scour hole widens laterally and correspondingly, the ridge also widens. This later formed wider ridge pushes forward the earlier formed narrow ridge downstream, resulting in the shape shown in Fig. 6c that is different from that noticed at larger H/b_o. Fig. 6d shows the normalised asymptotic perimeter of the ridge for a series of experiments having $F_o = 3.9$. One can note that all the data at higher tailwater conditions ($H/b_o \geq 4$) are closely spaced. The ridge is wider at $H/b_o = 1$ and non-symmetrical at low tailwater depths.

The asymptotic shape of the scour bed profiles for different densimetric Froude numbers (F_o) at $H/b_o = 18$ are presented in Fig. 6e. It can be seen that the depth and the distance of the maximum depth of the scour hole from the nozzle (x_m) increases with increasing F_o. Correspondingly, the height and location of the ridge increases with increasing F_o. Fig. 6f shows the profiles at three values of F_o for $H/b_o = 2$. At the lower value of F_o, the ridge crest is sharper while at $F_o = 10$, the ridge is flat and directly related to the prevailing local velocity (hence the shear stress). Fig. 6g shows the profiles at different F_o for $H/b_o = 1$. It is clear that the size and shape of the ridge is clearly dependent on densimetric Froude number (F_o) and tailwater depth. At very low tailwater depths, the ridge tends to be flat for all F_o.

Fig. 6h shows the variation of the ridge height with tailwater depth. With increasing tailwater depth, the ridge height increases quite rapidly and stabilizes to a near constant value beyond $H/b_o = 6$. Moreover, the effect of F_o is clearly distinct in the figure. Grain size has no significant effect on the relative height of the ridge at asymptotic conditions. It should be noted that at $F_o = 10$, the height of the ridge is slightly greater than the prevailing downstream depth of the flow at $H/b_o = 1$, which can also be found in the results of Ref. [9] for low H/b_o. Ref. [1] categorized the relative ridge height according to submergence. On re-interpretation of their data, one can note that at higher F_o (> 10), there is a critical tailwater depth beyond which an increase or decrease in tailwater depth causes an increase in ridge height.

Sediment deposition:

In the series of experiments conducted one could visually observe a differential deposition of fine and coarse particles at different locations in the scour hole and ridge. For example, fine particles were deposited at the side of the scour hole (see region "A" in inset of Fig. 7a). Also, coarser particles were noted at the bottom of the scour hole just downstream of the maximum scour depth. This layer of coarser particles was only about a grain size in thickness and is located between $0.55L_s$ to $0.75L_s$. This distribution of coarser particles resembles an "armoring layer" which forms when larger particles are

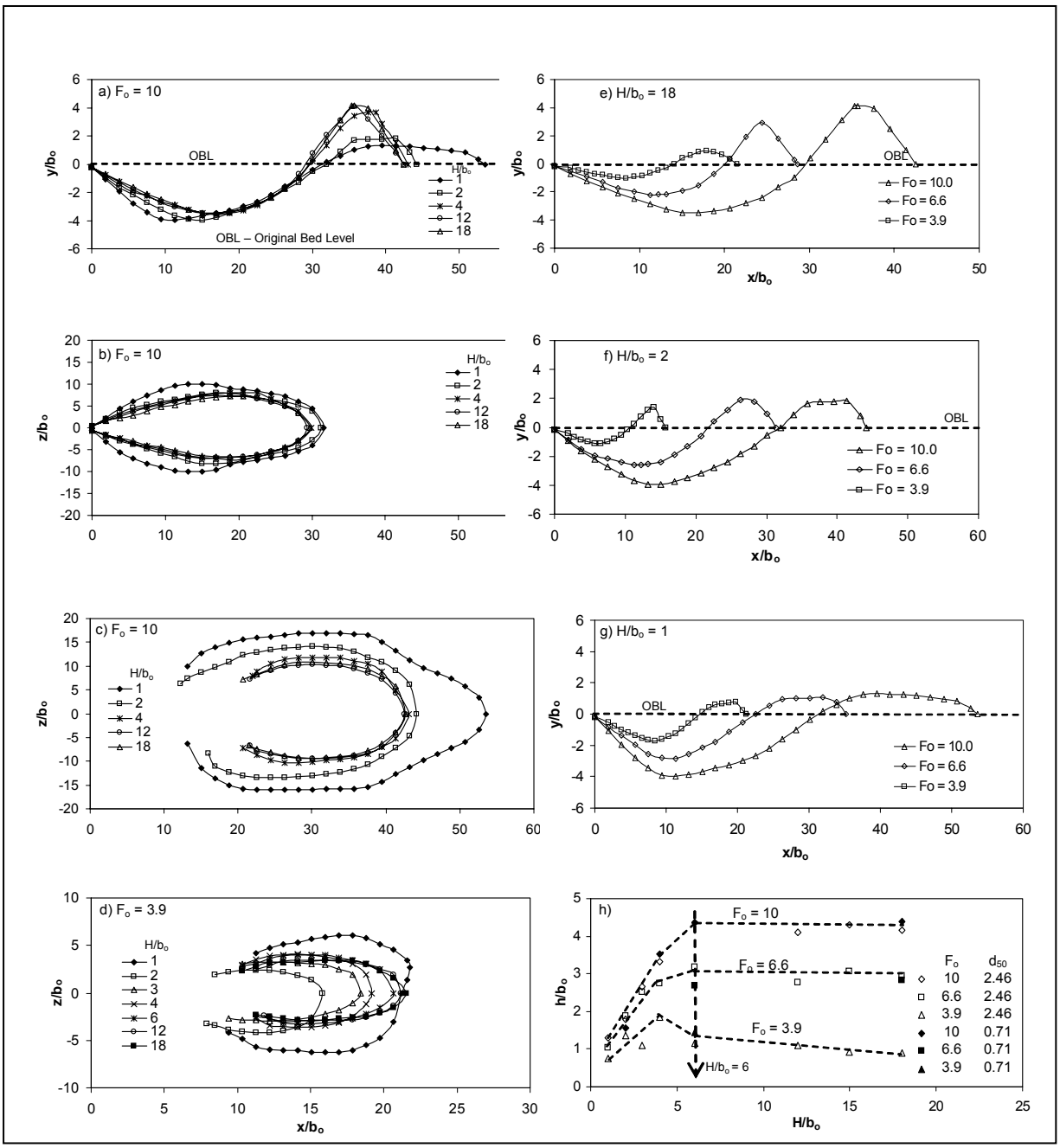

Fig. 6: Scour geometry at asymptotic conditions.

less susceptible to be transported (Ref. [7]). As the layer of sand is very thin and distributed over a small area, grain size sample was not collected from this region. The sand samples were collected for grain size analysis from three different locations, which are shown in an inset in Fig. 7a. Region "A" is the location where the fine particles are deposited. Region "B" is the downstream slope of the ridge and region "C" is the upstream slope of the ridge. Fig. 7a shows the result of sieve analysis of the experiments with $F_o = 10$ and $H/b_o = 2$. From this figure, one can note that the sand deposited on the downstream slope of the ridge is slightly coarser than that on upstream slope. This deposition pattern supports the earlier observation by Ref. [9]. A plausible explanation can be provided as follows. At the very beginning of the experiments, the fluid flows in a straight path and the particles tend to follow the fluid path due to the high jet momentum. With the gradual formation of the scour hole and the ridge, the fluid changes its straight path and follows a curvilinear path shown in the Fig. 7b. The larger particles, which are not able to follow the curvilinear path of the fluid because of their inertia, follow their original course and get transported straight up the ridge and then slide down. The relatively finer particles, which tend to follow the fluid more closely, get transported and deposited at the start of the ridge (zone "A"). Zone "A" also includes a part of the scour hole region and some finer particles are also observed on both the sides of the scour hole, which is caused by the sweeping motion originating in the turbulent burst.

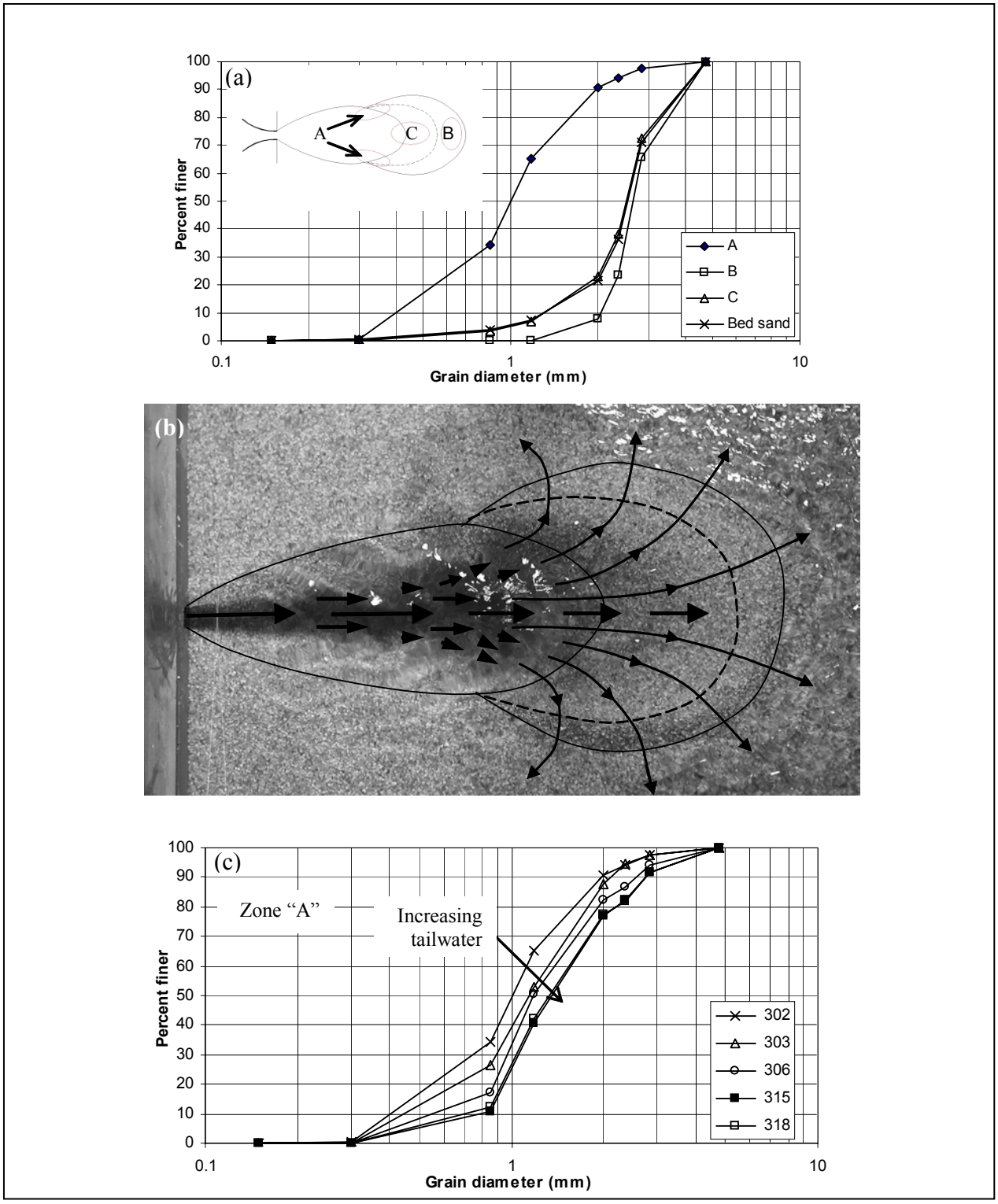

Fig. 7: a) Particle size distribution for Test no. 302, b) Curvilinear flow pattern near the ridge, c) Particle size distribution for experiments having different tailwater conditions.

Fig. 7c shows the particle size distribution at various tailwater depths in zone "A". The median diameter (d_{50}) of the fine particles increases with increasing tailwater depth and at high values of H/b_o, d_{50} remains nearly constant. At the low tailwater depths, dye visualization shows that the effect of the secondary flow becomes stronger. This enhances the scouring process of the sediment and results in the finest deposition at region "A". No systematic variation in grain size distribution with tailwater was observed for regions "B" and "C".

IV. Conclusions

The present study deals with local scour caused by three-dimensional square jets interacting with non-cohesive sand beds. The series of experiments cover a

range of tailwater conditions, densimetric Froude numbers and nozzle size-to-grain size ratios.

Previous studies have recognized that the densimetric Froude number (F_o) is the most important parameter that influences scour. The present study quantitatively identified the role of nozzle size-to-grain size ratio and tailwater depth. It has been observed that at a certain F_o, the evolution of scour with time depends on nozzle size-to-grain size ratio, however, at the asymptotic state, the scour hole parameters were found to be more-or-less independent of grain size. It was found that there is a dependence of maximum depth of the scour hole (ε_m) on tailwater depth but it is limited to $H/b_o \leq 1$ for $F_o = 3.9$, at $F_o = 6.6$ it is limited to $H/b_o \leq 2$, and at the highest value of F_o, the effect of tailwater is significant for $H/b_o \leq 3$. Tailwater was found to have a minimal effect on the maximum width of the scour hole. The length of the scour hole was found to be sensitive to the tailwater depth at shallower conditions. However, the trend at $F_o = 3.9$ is found to be different from that at higher values of F_o.

At an asymptotic state, the depth, width, and length of the scour hole initially decrease with increasing tailwater depth, and after a certain tailwater depth, the values tend to increase slightly and attain constancy. This effect is more prominent at low F_o. It should be noted that the trend seen in the present study is similar to earlier observation made by Ref. [2]. However, the changes with tailwater are not as prominent as that noted by them.

In an effort to provide useful but simplified scour predicting equations at asymptotic conditions, it was assumed that the role of grain size was completely absorbed by densimetric Froude number. The present data supports this assumption. The relationships for predicting the geometric parameters of the scour hole have been proposed in terms of densimetric Froude number (F_o) and tailwater depth. It has been found that the predictions based on the present study are more appropriate for a wide range of test conditions.

In this study, a differential deposition of fine and coarser particles at different locations in the scour hole and ridge was observed. Relatively coarser particles were transported in a straight path to downstream locations because of their larger inertia, whereas, the finer particles were carried by the secondary curvilinear flow around the ridge and were deposited on both the sides of the scour hole and also near the start of the ridge. The formation of migrating dunes and break up of the dunes by turbulent bursts was found to occur in the tests with the finer sand.

REFERENCES

[1] Ade, F. and Rajaratnam, N. (1998). "Generalized study of erosion by circular horizontal turbulent jets." *J. of Hydraulic Research, IAHR,* 36(4), 613-635.

[2] Ali, K. H. M. and Lim, S. Y. (1986). "Local scour caused by submerged wall jets." *Proc. of the Inst. of Civil Engrs.*, Part 2, 81, 607-645.

[3] Bey, A., Faruque, M. A. A. and Balachandar, R. (2005). "Two dimensional scour hole problem: Role of fluid structures." Submitted to the *J. of Hydraulic Engineering*.

[4] Chiew, Y. M. and Lim, S. Y. (1996). "Local scour by a deeply submerged horizontal circular jet." *J. of Hydraulic Engineering*, 122(9), 529-532.

[5] Faruque, M.A.A., Sarathi, P., and Balachandar, R. (2004). "Transient local scour by submerged three-dimensional wall jets: Effect of tailwater depth." *Second International Conference on Scour and Erosion, November 14 – 17, 2004, Singapore*, 2, 309-316.

[6] Lim, S. Y. (1995). "Scour below unsubmerged full-flowing culvert outlets." *Proc. of the Institution of Civil Engineers, Water Maritime and Energy*, 112(2), 136-149.

[7] Lim, S. Y. and Chin, C. O. (1992). "Scour by circular wall jets with non-uniform sediments." *Advances in Hydro-science and Engrg.,* 1, 1989-1994.

[8] Rajaratnam, N. and Berry, B. (1977). "Erosion by circular turbulent wall jets." *J. of Hydraulic Research*, 15(3), 277-289.

[9] Rajaratnam, N. and Diebel, M. (1981). "Erosion below culvert-like structure." *Proc., 5th Canadian Hydrotechnical Conf.,* May26–27, CSCE, 469-484.

[10] Sarathi, P. (2005). "Scour by submerged square wall jets at low densimetric Froude numbers." M. A. Sc. Thesis, Dept. of Civil and Environmental Engineering, University of Windsor, Ontario, Canada.